POLITECNICO DI TORINO
Repository ISTITUZIONALE

Photonic-integrated wavelength selective switch for S+C+L applications

(Article begins on next page)

19 April 2024

Photonic-integrated Wavelength Selective Switch for S+C+L applications

Lorenzo Tunesi[a], Ihtesham Khan[a], Muhammad Umar Masood[a], Enrico Ghillino[b],
Andrea Carena[a], Vittorio Curri[a], and Paolo Bardella[a]

[a]Politecnico di Torino, Corso Duca degli Abruzzi 24, Torino, Italy
[b]Synopsys Inc., Executive Blvd 101, Ossining, New York, USA

ABSTRACT

We propose a novel modular photonic integrated Wavelength Selective Switch (WSS) based on a reconfigurable optical multiplexer architecture, capable to operate over the S+C+L bands and scalable. The densely integrated solution takes advantage of an input stage with grating assisted contra-directional couplers to separate channels in the three considered communication bands, followed by a cascade of two-stage ladder ring resonators, to separating each transmitted channel. A final switching stage routes the signal to the desired output fiber, with a cascade of thermally controlled Mach-Zehnder interferometers. The transmission penalty of the proposed solution has been evaluated in a coherent transmission scenario.

Keywords: Multi-band Transmission, Optical Switching, PIC, Silicon Photonics, Wavelength Selective Switch.

1. INTRODUCTION

Today's optical transmission landscape is seeing a rapid increase in resource demand, due to bandwidth-intensive applications, emerging standards, such as 5G, and the expansion of the Internet of Things (IoT) paradigm. This requires an expansion of the current optical network infrastructure and capabilities, in order to accommodate the growing demand.[1] From the perspective of the network operator, two main solutions are available: new infrastructures can be deployed, which represents the expensive solution, or the residual capacity of the existing network can be exploited through multi-band paradigms, which represents the more cost-effective solution.[2] To achieve the full utilization of the remaining available fiber spectrum, new technologies such as Band-Division Multiplexing (BDM) must be enabled on top of the already existing Wavelength-Division Multiplexing (WDM) based network. This requires switching and filtering elements suited for an ultra-wide bandwidth of operation, allowing consistent performances in the whole needed spectrum. For this purpose, photonic integrated circuits (PICs) represent an ideal solution, as they provide a large bandwidth of operation while maintaining low footprint, cost, and power consumption. To this end, we propose a fully integrated modular wavelength-selective switch (WSS), able to independently route each of the input signal channels towards the desired output port, operating on the S+C+L optical transmission windows.

2. WSS ARCHITECTURE

The proposed WSS architecture achieves conflict-avoidance independent routing of the input channel by separating the switching and filtering operations into multiple stages, which are then cascaded into the desired configuration. This ensures the aforementioned modularity and scalability of the structure, as the design of each sub-stage can be tailored to the target implementation scenario. The general structure of the proposed architecture can be seen in Fig. 1; in the first section, the three bands of operation are filtered and routed to their respective channel filtering stage, which extracts the individual channels of the input WDM comb. After channel separation, each signal is then routed by an independent 1xN switching network, implemented as a cascade of fundamental 1x2 Optical Switching Elements (OSEs). After the switching section, an interconnect crossing stage links the output of the switches to their target output fiber. For our analysis, we designed and simulated the
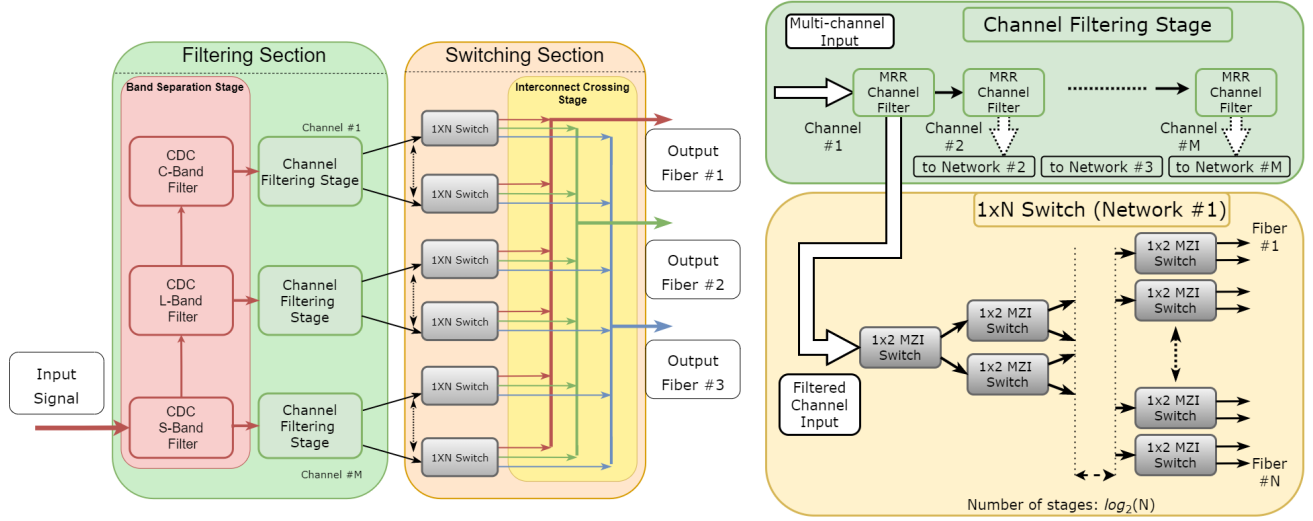

Figure 1: Proposed architecture for the WSS, highlighting the main functional blocks and their circuit representation.

device through the Synopsys Photonic Circuit Design Suite, considering a target implementation with 24 total channels (8 channels per band), with 3 possible output fibers. The simulation and design of the component has been carried out through different methods, ranging from BPM, FDTD simulations, CMT and analytical solutions: the waveguide and coupling simulations have been conducted in the Synopsys RSoft tool, allowing more detailed characterization of each sub-module, while the global simulation of the full device has been carried out in Optsim, which allows a block-oriented representation of the elements, and allowed the simulation of the whole structure at the transmission level, enabling a time-efficient and global evaluation of the implementation performance.

3. COMPONENTS DESIGN AND SIMULATION

The device has been designed considering the standard Silicon Photonic platform SOI, with reference Si on SiO_2 ridge waveguides with width W=550 nm and height H=220 nm. Three different components have been used to achieve the WSS operation, with their circuit schematic and transmission performance depicted in Fig. 2. Regarding the filtering section, Contra-Directional Couplers (CDCs) have been used to achieve the S+C+L band separation, due to their flat wideband of operation and steep filtering rolloff (Fig. 2a). The CDC have been designed using pitch chirp to extend and tailor the filtering bandwidth to the required regions[3]. For our implementation, the pitch of the three gratings (S, C, and L bands, respectively) has been designed as Λ =289 nm, 313 nm and 325 nm, with the chirp $\Delta\Lambda$= 20 nm, 8 nm and 18 nm. The physical dimensions of the two waveguides are equal in all three operating region with W1=570 nm, W2=430 nm, ΔW1=100 nm, ΔW2=60 nm, with gap G=200 nm. The length of the three components are L=2.6 mm, 1.2 mm and 1 mm respectively, with the resulting frequency response highlighted in the figure. For the next stage of filtering, a different filtering component is used to avoid the large footprint that CDCs introduce. After the band separation, the channel extraction is carried out by a cascade of two-stage ladder MicroRing-Resonator (MRR) filters. The MRR radius is designed in order to obtain the desired frequency response for the target 100 GHz spaced WDM comb[4]. One issue that arises from the use of resonator-based filtering elements is the channel aliasing, which would rapidly degrade the performance by introducing large insertion losses and crosstalk. This is mitigated by modelling the MRR elements with grating-assisted coupling structure instead of the traditional directional coupler[5]: as illustrated in Fig. 2b, the filters can be designed to operate as Free Spectral Range (FSR) free elements, avoiding the otherwise severe channel aliasing. This allows a better scalability with respect to the traditional solutions, which would require multiple stages of filtering designed at different FSR, as to select only a single channel between the images[6]. After the filtering stage, the OSE have been implemented as MZI thermally controlled 1x2 switches (Fig. 2c). These elements provide a flat and large bandwidth for the desired application[7], depicted in Fig.2 for

(a) CDC band filter. (b) Two-stage ladder channel filter. (c) MZI switching element.
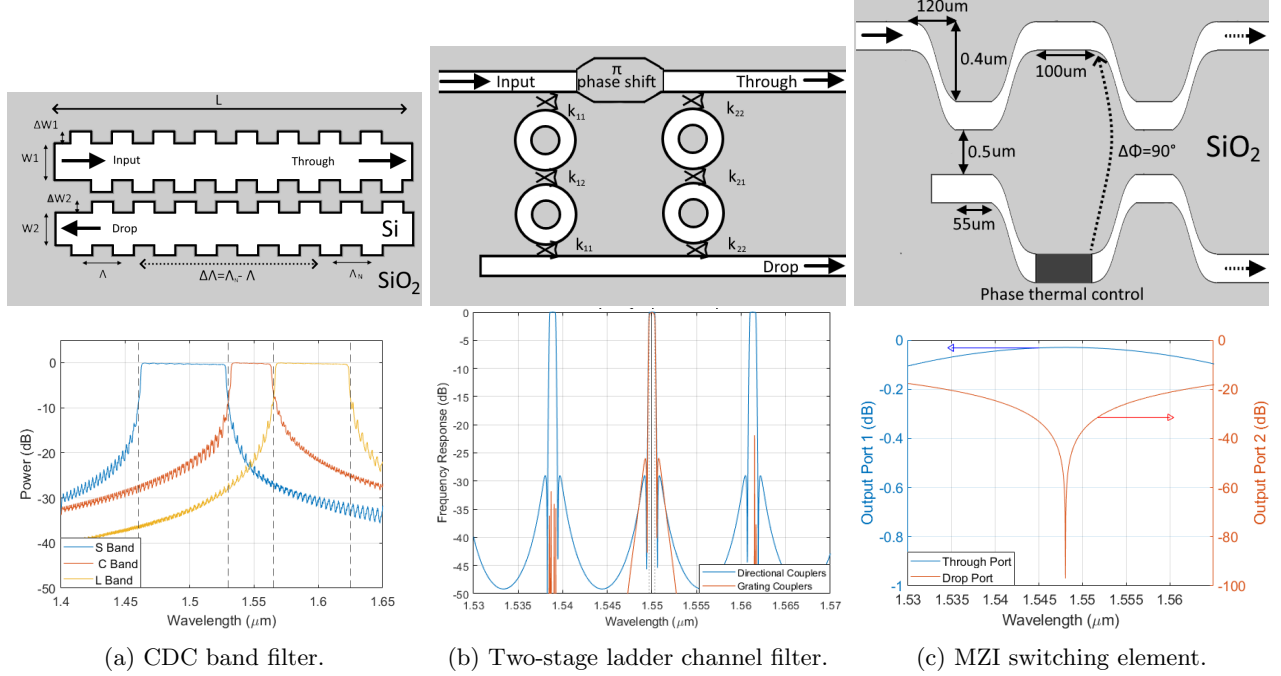
Figure 2: Main devices circuit representation and transmission performances

operation in the C band. In each switching subnetwork the MZI design can be tuned to provide the maximum transmission, while reducing the distortion and filtering penalties. The following interconnect crossing network has been modelled considering each waveguide crossing as a lossy element, introducing 0.06 dB of loss in the considered spectrum, which is comparable state of the art crossing technologies[8, 9].

Furthermore the waveguide combiner used in the interconnect stage have been modeled under a similar assumption, considering the insertion losses reported in the literature for optimized integrated wavelength combiners.[10, 11]

4. RESULTS AND CONCLUSIONS

The structure has been simulated in a coherent transmission scenario, considering dual-polarization 16QAM modulation, with a symbol rate Rs=60 GBaud and spacing FSR=100 GHz. The added penalty for optical signal-to-noise ratio (OSNR) has been considered as the performance metric to characterize the impairment of the device's quality of transmission (QoT). This metric has been evaluated by simulating the Bit-Error Rate (BER) for the different routings of all the possible channels, comparing it with the back-to-back BER of the transmitter-receiver system: the OSNR penalties have been extracted for a target BER of 10^{-3}. The results of these simulations are depicted in Fig. 3, highlighting separately the OSNR penalty and the estimated insertion losses. In Fig. 3a the added penalty is depicted as a function of the number of waveguide crossings encountered, as this represents the path-dependent effect based on the required routing. In Fig. 3b the chip insertion losses are depicted for the eight channels under analysis, as for the proposed configuration this represents a path-independent fixed power loss: the values for the insertion losses have been simulated based on Table 1, which considers reasonable values available in the literature.

Component	Through port	Drop port
MMI[10]	0.50	–
MRR[12]	0.35	0.85
MZI[13]	0.32	–
CDC[3]	0.25	0.70

Table 1: Reference value for the insertion losses of the main components (expressed in decibel).
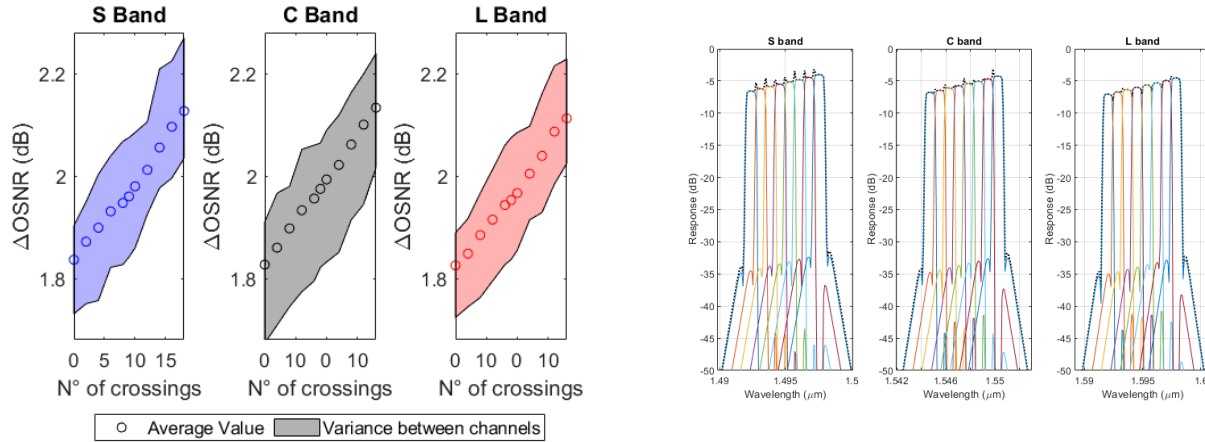
(a) OSNR Penalties

(b) Transmission spectrum and insertion losses

Figure 3: (a) Results of the transmission simulation highlighting the path-dependant OSNR penalties and (b) the fixed losses introduced by the elements cascade.

Overall, the design strategy and the proposed architecture show promising results, with a large operating bandwidth that can independently handle each channel of the WDM comb, without introducing severe filtering penalties on the channels and maintaining reasonable insertion losses.

REFERENCES

[1] Cisco, "Cisco annual internet report (2018–2023) white paper," (2020).

[2] Curri, V., "Multiband optical transport: a cost-effective and seamless increase of network capacity," in [*OSA Advanced Photonics Congress 2021*], *OSA Advanced Photonics Congress 2021* , NeTu2C.3, Optical Society of America (2021).

[3] Hammood, M., Mistry, A., Yun, H., Ma, M., Lin, S., Chrostowski, L., and Jaeger, N. A. F., "Broadband, silicon photonic, optical add–drop filters with 3 dB bandwidths up to 11 THz," *Opt. Lett.* **46**, 2738–2741 (Jun 2021).

[4] Masilamani, A. P. and Van, V., "Design and realization of a two-stage microring ladder filter in silicon-on-insulator," *Opt. Express* **20**, 24708–24713 (Oct 2012).

[5] Eid, N., Boeck, R., Jayatilleka, H., Chrostowski, L., Shi, W., and Jaeger, N. A. F., "Fsr-free silicon-on-insulator microring resonator based filter with bent contra-directional couplers," *Opt. Express* **24**, 29009–29021 (Dec 2016).

[6] Tunesi, L., Khan, I., Masood, M. U., Ghillino, E., Carena, A., Bardella, P., and Curri, V., "Novel design and operation of photonic- integrated wss for ultra-wideband applications," in [*2022 IEEE Photonics Society Summer Topicals Meeting Series (SUM)*], 1–2 (2022).

[7] Khan, I., Tunesi, L., Masood, M. U., Ghillino, E., Bardella, P., Carena, A., and Curri, V., "Performance evaluation of data-driven techniques for softwarized and agnostic management of N×N photonic switch," *Opt. Continuum* **1** (Jan 2022).

[8] Yi, D., Zhou, W., Zhang, Y., and Tsang, H. K., "Inverse design of multi-band and wideband waveguide crossings," *Opt. Lett.* **46**, 884–887 (Feb 2021).

[9] Wu, S., Mu, X., Cheng, L., Mao, S., and Fu, H., "State-of-the-art and perspectives on silicon waveguide crossings: A review," *Micromachines* **11**(3) (2020).

[10] Singh, S., Kojima, K., Koike-Akino, T., Wang, B., Parsons, K., Nishikawa, S., and Yagyu, E., "An MMI-based wavelength combiner employing non-uniform refractive index distribution," *Opt. Express* **22**, 8533–8540 (Apr 2014).

[11] Mu, J., Vázquez-Córdova, S. A., Sefunc, M. A., Yong, Y.-S., and García-Blanco, S. M., "A low-loss and broadband MMI-based multi/demultiplexer in Si_3N_4/SiO_2 technology," *J. Lightwave Technol.* **34**, 3603–3609 (Aug 2016).

[12] Popovíc, M. A., Barwicz, T., Watts, M. R., Rakich, P. T., Socci, L., Ippen, E. P., Kärtner, F. X., and Smith, H. I., "Multistage high-order microring-resonator add-drop filters," *Opt. Lett.* **31**, 2571–2573 (Sep 2006).

[13] Zhao, S., Lu, L., Zhou, L., Li, D., Guo, Z., and Chen, J., "16×16 silicon Mach–Zehnder interferometer switch actuated with waveguide microheaters," *Photon. Res.* **4**, 202–207 (Oct 2016).